Reconstituting the Interaction Between Purified Nuclei and Microtubule Network

Gökçe Agsu, Jérémie Gaillard, Bruno Cadot, Laurent Blanchoin, Emmanuelle Fabre, Manuel Théry

Reconstituting the interaction between purified nuclei and microtubule network

G. Agsu, J. Gaillard, B. Cadot, L. Blanchoin, E. Fabre, M. Théry

ABSTRACT

Nucleus gets deformed during cell migration, stem cell differentiation or senescence. While comprehensive work has been accomplished in cells to assess the role of nuclear deformations, this approach is considered intrinsically limited due to the undistinguishable impact of infinite number of soluble factors, molecules, or proteins present in cells. It is therefore important to reconstitute *in vitro* nuclear deformations and this requires nuclei with intact nuclear envelope free from plasma membrane. In this method we describe a nucleus purification protocol that is suitable for non-adherent cells and provide evidence on elimination of cell membrane and the undamaged state of the nuclear envelope. We also show that purified nuclei can specifically interact with microtubules, and recapitulate microtubule interaction. This protocol allows the study of MT-nucleus interaction *in vitro*.

1. Introduction

Nucleus has been suggested to be the stiffest organelle in the cell, and yet its shape can change during stem cell differentiation [1] (Biedzinski et al, 2020), cancer cell transformation [2] (Zink et al, 2004), epithelial to mesenchymal transition [3] (Legget et al, 2016), laminopathy induced senescence [4,5] (Sullivan et al, 1999; Scaffidi and Misteli, 2006), nuclear import of YAP/TAZ (Cosgrove et al, 2021), nuclear mechanosensing [6] (Nava et al, 2020) release of neutrophil extracellular traps [7] (also known as NETosis; Brinkmann et al, 2004), endothelial barrier crossing of leukocytes [8] (Barzilai et al, 2017) and confined cell migration [9] (Thiam et al, 2016).

In adherent cells, actin filaments regulate nuclear deformations. Dorsal actin cables apply forces on the nucleus with the involvement of focal adhesions and actomyosin network through the linker of nucleoskeleton and cytoskeleton (LINC) complex [10-14] (Makhija et al, 2015; Kim and Wirtz, 2015; Cheng et al, 2016; Buxboim et al, 2017; revised in Davidson & Cadot 2020). Microtubules (MTs) are also known to interact with nuclei during nuclear positioning and rotation [15-18] (Starr & Fridolfsson 2010; Reinsch & Gönczy 1998; Cadot *et al,* 2012; Renkawitz *et al,* 2019) with the help of motors [19,20] (Metzger et al, 2012; Gache et al, 2017), nuclear membrane fluctuation [21] (Almonacid *et al,* 2019), as well as DNA double strand break mobility and repair [22] (Lottersberger *et al,* 2015). Additionally, in contrast to adherent cells, it seems to be MTs that regulate nuclear deformations in non-adherent cells. This has been documented in two independent studies on early [1](Biedzinski *et al,* 2020) and terminal differentiation [23] (Olins & Olins 2004) of blood cells in humans. Former study shows that, during hematopoietic stem cell (HSC) differentiation into common myeloid progenitors (CMP), MT network reorganizes to form bundles along the nuclear membrane and deforms the nucleus by deep invaginations that result in chromatin remodeling and in alteration of the transcriptional program [1](Biedzinski *et al,* 2020). Similarly, human cytomegalovirus (CMV) infection is also able to orchestrate nucleus deformation using MT forces [23] (Procter *et al,* 2020). When infected a cell, CMV triggers *de novo* microtubule organizing center (MTOC) production, which polymerizes MTs binding to nuclear-bound dynein that results in the polarization of the nuclear envelope (NE) proteome. This viral-induced mechanical cascade causes nucleus deformation with consequences on chromatin architecture that eventually enhances the viral replication in the cell [23] (Procter *et al,* 2020).

As exemplified above, there are many parameters that regulate the nucleus shape. Reconstitution *in vitro* appears preferable to study the specific parameter of interest, because it avoids unknown effects of the components of a crowded cytoplasm. Such reconstitution assay requires nucleus purification protocol that preserves the NE intact. Previous nucleus purification protocols for adherent cells include cell scraping, a step that contributes to cell shearing and to purification yield, which cannot be applied to non-adherent cells [24,25] (Guilluy *et al,* 2014; Stephens et al, 2017). It is therefore necessary to develop a nucleus purification protocol to remove cell membrane without damaging the NE in non-adherent cells. In the past, nuclei have been purified with detergents from non-adherent lymphocytes with the aim of studying the centrosome-nucleus association [26] (Maro & Bornens, 1980). This detergent-based protocol results in high yield of purified nucleus. However, in reconstitution assay it is essential to keep NE structure as native as possible. Therefore it is preferable to avoid detergent treatments.

Here, we describe a nucleus purification protocol dedicated to non-adherent cells that allows to purify nuclei free of plasma membrane with intact NE. We also describe a reconstitution assay in buffer conditions that are compatible with gliding assay where kinesin-1 motors and nucleus-bound dynein compete for MT interaction. This method enables recapitulating *in vivo* phenotype of MT-nucleus interaction as well as monitoring the MT network around the nucleus.

2. Methods

2.1 Flow chamber fabrication

In this part, we describe a low-cost protocol to fabricate flow chambers. It can be easily performed with commonly found materials in laboratories.

Materials

i. Reagents

- NaOH 1M
- EtOH 96%
- MilliQ water

ii. Equipment

- Cover slip (thickness: 1, 20 x 20 mm, Knittel Glass)
- Microscope slides (3 x 1 inch, Knittel Glass)
- Coverslip mini-rack
- Slide mini-rack
- Double tape spacer (thickness: 70µm)
- Metallic tweezers to handle glass coverslips
- Glass beaker for washing and stocking clean coverslips
- Parafilm
- Sonicator

Protocol

- Place coverslips and microscope slides in their special mini-racks and place them in glass beakers. Fill the beakers with 1M NaOH.

- Cover the top of the beakers with parafilm and sonicate for 30 min.
- Discard NaOH solution and fill the beakers with MilliQ 3 times.
- Discard the MilliQ and fill the beakers with 96% EtOH in order to wash for 30 min.

Remark: Coverslips and slides can be stored in EtOH in tightly sealed containers for up to one week.

- Wash the coverslips and slides one by one sequentially in 3 MilliQ buckets with the help of tweezers.
- Assemble the flow chamber with one dry coverslip and one dry slide using a double-sided tape spacer to create a channel.

Remark: Protein coating yield and quality will depend on the cleanliness of the coverslips. Therefore, assembly of the flow chamber should be performed on the day of experiment.

Remark: Protect the flow chamber from dust and store in a box before usage. Seal the box with parafilm.

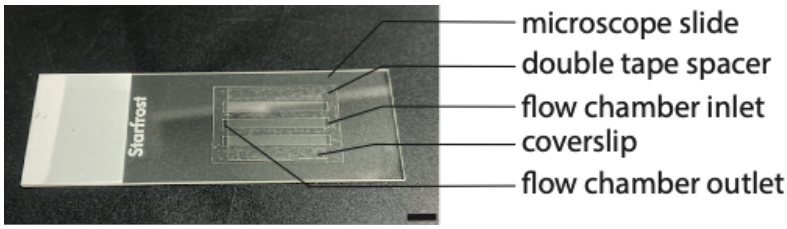

Figure 1. Assembled flow chamber. scale bar 500mm

2.2 Microtubule polymerization and taxol stabilization

In this section we give instructions of MT polymerization *in vitro* [27] (Triclin et al. 2021) and taxol stabilization.

Materials

i. Reagents

- Tubulin: Systematically purified and labeled in our lab as described in Schaedel et al., 2015. Briefly, tubulin was purified from fresh bovine brain by three cycles of temperature-dependent assembly and disassembly in Brinkley Buffer 80 (BRB80 buffer; BRB buffer: 80 mM PIPES, pH 6.8, 1 mM EGTA, and 1 mM $MgCl_2$ plus 1 mM GTP) [(40)] [27]. MAP-free neurotubulin was purified by cation-exchange chromatography (EMD SO, 650 M, Merck) in 50 mM PIPES, pH 6.8, supplemented with 1 mM $MgCl_2$, and 1 mM EGTA [(41)] [28]. Purified tubulin was obtained after a cycle of polymerization and depolymerization. Fluorescent tubulin (ATTO-565-labeled tubulin) was prepared as previously described [(42)] [29]. Microtubules from neurotubulin were polymerized at 37°C for 30 min and layered onto cushions of 0.1 M NaHEPES, pH 8.6, 1 mM $MgCl_2$, 1 mM EGTA, 60% v/v glycerol, and sedimented by high centrifugation at 30°C. Then Microtubules were resuspended in 0.1 M NaHEPES, pH 8.6, 1 mM $MgCl_2$, 1 mM EGTA, 40% v/v glycerol and labeled by adding 1/10 volume 100 mM NHS-ATTO (ATTO Tec) for 10 min at 37°C. The labeling reaction was stopped using 2 volumes of 2X BRB80, containing 100 mM potassium glutamate and 40% v/v glycerol, and then Microtubules were sedimented onto cushions of BRB80 supplemented with 60% glycerol. Microtubules were resuspended in BRB80, and a second cycle of polymerization and depolymerization was performed before use.

Remark: Avoid using tubulin stocks older than 4-6 months as they are less efficient in MT polymerization.

- BRB80: 80 mM PIPES, pH 6.8, 1 mM EGTA and 1 mM MgCl2
- Taxol (Sigma)
- GTP (Sigma)
- DMSO
- MgCl2
- MilliQ H2O

ii. Equipment

- Eppendorf tubes 500µL
- Thermo-mixer suitable for Eppendorf tubes
- Aluminum foil

Protocol

As previously described in Triclin *et al* 2021. Briefly,

- Prepare tubulin premix in BRB80 1X by supplementing it with MgCl2 (20mM) and GTP (5mM) and 1/4 volume of DMSO. Keep it at RT.
- Prepare taxol buffer (10µM) in BRB80 0.5X. Keep it at RT.
- Prepare tubulin mix (70µM) with 20% illumination (20% ATTO565-labeled tubulin and 80% non-labeled tubulin) in BRB80 1X.
- Set hot plate at 37°C
- Initiate the microtubule polymerization by adding 1 volume of tubulin premix to 4 volumes of tubulin mix within an Eppendorf tube. Mix by gentle tapping.
- Place the tube in thermo-mixer and incubate for 30 min.

Remark: Longer incubation time yields in longer MTs.

- Stabilize the MT polymerization by adding half volume of taxol buffer and mix by gentle tapping. (Figure 2)
- Protect from light with aluminum foil wrap and keep at RT.

Remark: Avoid harsh pipetting and always cut pipette tips before pipetting in order to prevent MT breakage.

Remark: Every batch of newly-polymerized taxol-stabilized microtubules can be stored up to 3 or 4 days at RT. During storage, MT annealing will take place and this will result in longer MTs in time.

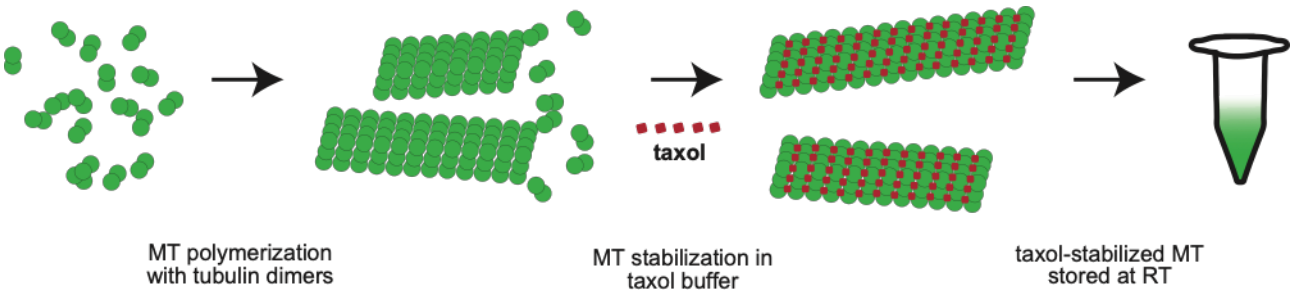

Figure 2. MT polymerization and taxol stabilization. MT polymerization is initiated with initially purified and fluorescent-labeled tubulin dimers in BRB80 buffer at 37°C for 30 minutes. When MTs reach sufficient

length (20 - 30µm of length after around 30 min of polymerization in the above mentioned biochemical conditions), the polymerization process is stopped upon taxol addition.

2.3 Purification of intact nucleus from non-adherent cells

In this section, we describe a hypotonic shock-based nuclei purification protocol that has been adapted for non-adherent HSCs and immortalized human T lymphocytes, Jurkat cells. This protocol allowed us to preserve the dynein population that is bound to the NE in both of the cell types.

Materials

i. Reagents

- Sterile PBS
- Hypotonic buffer: 9mM Hepes pH 7.4, 0.9mM KCl, 1.35mM $MgCl_2$, 0.5mM dithiothreitol, 1% protease inhibitor cocktail, 10% IMDM medium
- Sucrose buffer: 20mM Hepes pH 7.4, 25mM KCl, 5mM $MgCl_2$, 0.25M sucrose, 100mM ATP, 10µg/mL Hoeschst
- MilliQ

ii. Equipment

- Dounce homogenizer 2mL
- Vortex
- Centrifuge
- Falcon tubes 15mL
- Kimtech wipes

Protocol

Remark: HSCs are isolated from human cord blood through CD34 selection as described in Biedzinski *et al*. 2020. Briefly, all human umbilical cord blood samples collected from normal full-term deliveries were obtained after mothers' written and informed consent, following the Helsinki's Declaration and Health Authorities. Cord blood samples came from the biological resource center, Saint-Louis Hospital Cord Blood Bank (Paris, France) authorized by French Cord Blood Network (AC 2016-2756, French Biomedical Agency, Paris, France). Mononuclear cells were collected using Ficoll separation medium (Eurobio, Courtaboeuf, France). CD34+ cells were further selected using Miltenyi Magnetically Activated Cell Sorting (MACS) columns (Miltenyi Biotech, Paris, France) according to the manufacturer's instructions. CD34+ cells were then either put in culture or frozen at -80°C in IMDM medium (Gibco) supplemented with 10% fetal bovine serum (FBS) and 10% DMSO (WAK Chemie Medical GmbH). Freshly isolated CD34+ or thawed cells were allowed to recover overnight at 37°C in IMDM medium supplemented with 10% FBS and antibiotics (Antibiotic-antimycotic, Sigma-Aldrich).

- Collect 1mL (nearly 500K cells) CD34+ HSCs or Jurkats in a falcon tube that contains 4mL PBS.

Remark: Purification protocol on non-adherent cells doesn't require initial cell scraping, thanks to which the protocol is less destructive. However, hypotonic shock requires optimization depending on the cell type. For instance, in an initial study, hypotonic-shock based nucleus purification for HeLa cells required a stronger hypotonic shock (Guilluy *et al,* 2014), whereas in our protocol HSCs and Jurkats should be treated in milder hypotonic conditions.

- Centrifuge at 244 g for 5 min.
- Remove the supernatant, keep the pellet and resuspend it in 5mL PBS.
- Centrifuge at 244 g for 5 min.
- Remove the supernatant by inverting the falcon tube upside down carefully and drying the tip with Kimtech wipe.
- Add 500µL hypotonic buffer to the pellet, resuspend immediately and transfer it in the homogenizer container incubated in ice.
- Incubate on ice for 5 min.
- Apply 30 up/down strokes with the glass grinder (Figure 3)
- Transfer the liquid in a pre-cooled 1.5mL eppendorf tube.
- Centrifuge at 500 g for 5 min at 4°C. (Figure 3)
- Eliminate the supernatant by inverting the eppendorf tube on a Kimtech wipe and wash again with 500µL hypotonic buffer.
- Gently vortex for 2s.
- Centrifuge at 500 g for 5 min at 4°C. (Figure 3)
- Eliminate the supernatant and use again a kimtech wipe in order to completely remove the remaining liquid in the eppendorf tube.
- Add 100µL sucrose buffer and gently resuspend the pellet.

Remark: Pipette tip must be cut to prevent damage on the nucleus.

- Purified nuclei can be stored in ice for up to 3 hours. Do not freeze and thaw.

Figure 3. Nucleus purification principles and results. **A.** Illustration of purification method. Non-adherent HSCs or Jurkats are collected and resuspended in hypotonic buffer in order to render cell membrane more fragile to mechanical shearing. After 5 minutes of incubation on ice, cell membrane is mechanically sheared upon 30 up and down homogenizer strokes. Next, serial centrifugation is performed in order to remove the cytoplasm and cell membrane remnants. Small pellet of isolated nuclei is resuspended in sucrose buffer and kept on ice for up to 3 hours. **B.** Nuclear envelope in the course of purification **C.** Cell/nucleus ratio after given rounds of homogenizer strokes. Plateau suggests 30 is optimal. **D.** General comparison of cell and nuclei before and after the purification, respectively. **E.** Detailed representation of nucleus purification yield on HSC and Jurkat cells. **F.** amount of centrosome-bound nuclei in the course of purification. We observe a sharp decrease after homogenization, where only 15% of the nucleus still bear centrosome. Pre-treating cells with taxol doesn't ameliorate the percentage (15% for pre-taxol samples). (**B** and **E**: scale bar, 5µm.) (**D**: scale bar, 10µm.) **HSC**: hematopoietic stem cell.

2.4 Reconstitution of nucleus - microtubule interaction in bulk

In this step, we describe how to assemble taxol-stabilized MTs and purified nuclei together. This step requires proper biochemical conditions where nuclei don’t shrink due to high salt concentration of the MT buffer and MTs remain stabilized in final taxol concentration of 10µM.

Materials

i. Reagents

- Polymerized and taxol-stabilized MTs prepared in section 2.2 (hereafter named MT stock)
- Purified HSC or Jurkat nuclei prepared in section 2.3 (hereafter named nuclei)
- Saturation buffer at RT: 1% w/v BSA in HKEM (10 mM HEPES pH=7.2, 50 mM KCl, 1 mM EGTA, 5 mM MgCl2)

- Wash buffer at RT: 10 mM HEPES, 16 mM PIPES (pH 6.8), 50 mM KCl, 5 mM MgCl2, 1 mM EGTA, 20 mM DTT, 3 mg/ml glucose, 20 µg/ml catalase, 100 µg/ml glucose oxidase, and 0.3% BSA supplemented with 10µM taxol
- ATP buffer on ice until usage: 10 mM HEPES, 16 mM PIPES (pH 6.8), 50 mM KCl, 5 mM MgCl2, 1 mM EGTA, 20 mM DTT, 3 mg/ml glucose, 20 µg/ml catalase, 100 µg/ml glucose oxidase, 0.3% BSA, 8 mM ATP, and 0.2% Methyl cellulose supplemented with 10µM taxol

ii. Equipment

- Freshly assembled flow chambers
- Kimtech wipes (or whatman paper)
- Valap sealant (pre-warmed mixture of equal weight of vaseline, lanolin, and paraffin)

Protocol

Remark: Asses the inlet and the outlet of the flow chamber before introducing the fluids (Figure 1). Always introduce buffers using the same flow chamber inlet and apply flow in the same direction. Perform each wash step upon capillary action by introducing the wash buffer in the inlet and by placing a kimtech wipe or whatman paper in the outlet.

- Add 5µL of saturation buffer into the flow chamber and incubate for 3 minutes. Wash the flow chamber with 5µL of wash buffer.
- Mix 3µL of MT stock with 47µL of wash buffer. The aim is to dilute the amount of MTs added in the chamber to track individual MTs more easily.

Remark: Cut the pipette tip before pipetting MTs or nuclei.

- Mix 10µL of diluted MTs, 10µL of nuclei and 10µL of ATP buffer in a new eppendorf tube.
- Immediately load 10µL of the mix in the flow chamber.

Remark: Avoid serial loading of purified elements. Co-incubate and co-load nuclei, MTs and ATP buffer in order to make sure that nuclei are not washed off, that MTs are not broken due to multiple fluid flows, or that the ATP buffer is not diluted.

- Once sealed, put the flow chamber in the microscope's pre-heated incubator at 37°C and initiate image acquisition. We acquired images of the full nucleus stack every 15 seconds for 30 minutes on Nikon spinning disk confocal microscope.

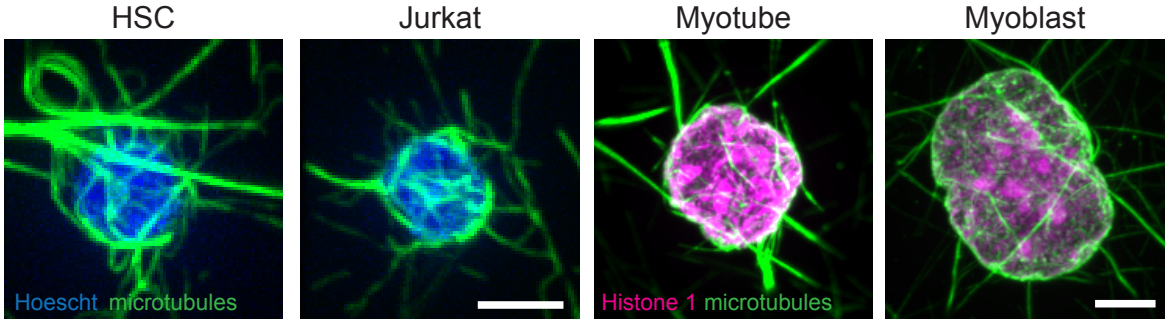

Figure 4. MT network interacts with purified nuclei from various non-adherent and adherent cell lines. (scale bar 5µm)

When co-loaded in the flow chamber, taxol-stabilized MTs and purified nuclei were able to interact in 3D upon bundling and buckling along the nuclear membrane (Figure 4, HSC and Jurkat). In order to validate the reproducibility of our MT-nucleus interaction reconstitution method, we tested

our protocol on nuclei purified from different cell types, including adherent mouse myoblast and myotube cells (CADOT REFERENCE Dean & Kasamatsu, 1994 JBC). When we used the reconstitution protocol on purified myoblast and myotube nuclei with same amount of MTs, we could recapitulate similar interaction and buckling events all around the nuclei (Figure 4, myotube and myoblast). This suggests that MT-nucleus crosstalk reconstitution assay can also be applied on adherent cell nuclei.

2.5 Reconstitution of nucleus - microtubule interaction in motility context:

Next, we established reconstitution *in vitro* in the context of gliding assay where kinesin-1 is coated on the clean glass surface of the flow chamber. Kinesin-1 coating was important to ensure that buffer conditions were compatible for molecular motor functioning. It also set a competition between nucleus-bound dynein and coated kinesin-1 for MT interaction.

Materials

i. Reagents

- MT stock and nuclei stock used in section 2.4.
- Saturation buffer, wash buffer, ATP buffer used in section 2.4.
- 200 nM GFP-tagged kinesin-1 in Wash buffer on ice. Truncated kinesin-1 motor protein was purified using bacterial expression as previously described (Pierce & Vale, 1998). Plasmid for the kinesin construct, pET17_K560_GFP_His, was purchased from Addgene (15219, Cambridge, MA). Recombinant, truncated kinesin-1 motor protein fusion proteins were transfected into Rosetta2 (DE3)-pLysS E. coli (VWR) and expression was induced with 0.2 mM IPTG for 16 h at 20°C. Harvested cells were resuspended in buffer A (50 mM sodium phosphate buffer pH 8, 250 mM NaCl) containing 0.1% Tween-20, 0.5 mM ATP and 3 protease inhibitors (Roche) and lysed by sonication. The lysates were centrifuged 30 min at 25000 g and 4°C. We add 20 mM Imidazole to the clear lysates and were loaded onto a NiSepharose HP column (GE Healthcare). The column was washed with buffer B (50 mM sodium phosphate buffer pH 6, 250 mM NaCl, 1 mM MgCl2, 0.1 mM ATP). Proteins were eluted in buffer C (50 mM sodium phosphate buffer pH 7.2, 250 mM NaCl, 500 mM Imidazole, 1 mM MgCl2, 0.1mM ATP) then desalted into PEM-100 buffer containing 0.1 mM ATP, and snap-frozen in liquid nitrogen.
- Anti-GFP antibody (Invitrogen) at 0.2 mg/mL on ice.

ii. Equipment

- Identical as section 2.4.

Protocol

- Add 5µL of Anti-GFP antibody into the flow chamber and incubate for 3 minutes. Wash the flow chamber with 5µL of saturation buffer.
- Add 5µL of GFP-tagged kinesin-1 in the flow chamber and incubate for 3 minutes. Then, wash with 10µL wash buffer.
- Mix 3µL of MT stock with 47µL of wash buffer. The aim is to dilute the amount of MTs added in the chamber to track individual MTs more easily.
- Mix 10µL of diluted MTs, 10µL of nuclei and 10µL of ATP buffer in a new eppendorf tube.
- Immediately load 10µL of the mix in the flow chamber.

- Seal the flow chamber with valap (or any other equivalent sealing material) and initiate immediate image acquisition as described in section 2.4.

Figure 5. *in vitro* reconstitution of MT networks with purified HSC and Jurkat nuclei. **A.** Selective interaction of MTs with HSC nuclei (lower panel). MTs interacted less efficiently with intact HSC (upper panel). **B.** MT-nucleus interaction from various angles. During the imaging, we were able to follow the dynamic MT-nucleus interaction in 3D during which MTs climbed over the purified nucleus and framed it upon bundling and buckling (red asterix). Side view reconstructed images are interpolated. **C.** Mean intensity of MT fluorescence on the nucleus surface in time. n=2 (6 nuclei for co-loaded condition, 4 nuclei for sequentially loaded condition) **D.** Carboxylated beads do not interact with motor-mobilized MTs. This points at the specificity of MT-nucleus interaction shown in panel B. **E.** Motility of MTs in time with color code. Image taken every 15 seconds. (scale bar 5µm)

We co-loaded taxol-stabilized MTs with purified nuclei and intact cells in the flow chamber (Figure 5A). Live-imaging revealed that MTs didn't specifically interact with intact cells (Figure 5A, upper panel and Figure 5B). Oppositely, we observed that MTs associated and specifically interacted with purified nuclei (Figure 5A, lower panel). Within 30 minutes of imaging, we observed a significant increase in the intensity of the MT network established around the nucleus. (Figure 5B, 5C). Once interacted with the purified nuclei, MTs remained buckled around it (Figure 5B) by making bundles along the nuclear membrane and by surrounding them upon 3D interaction (Figure 5B, red asterix).

In the protocol section 2.4, it's not recommended to do serial loading of purified elements in order to avoid nuclei being flushed out of the flow chamber. However, we tested the result of serial loading in our experimental work in order to illustrate the difference of MT-nucleus interaction between the options of co-loading and serial loading of purified elements. When added separately, MTs and nuclei have less interaction in time (Figure 5C). Next, in order to show the specificity of MT-nucleus interactions, we repeated the same protocol by pre-incubating the same amount of MTs with nucleus-sized beads (10µm) and by co-loading the mix into the flow chamber. During the live imaging, MTs remained completely mobile in the flow chamber and continued gliding on a kinesin-1-coated surface (Figure 5D, Figure 5E, right). Temporal analysis of MT gliding behavior revealed that HSC nuclei outcompeted kinesin-1 in MT-interactions and strongly associated with MTs (Figure 5E, left). Oppositely, MTs gliding near beads neither interacted with nor accumulated around them (Figure 5E, right).

3. Discussion

We describe a method to study MT-nucleus interaction in a reconstitution assay. For this purpose, we first established a nucleus purification protocol for non-adherent cell types. With cell membrane staining, we could show the plasma membrane was eliminated in HSCs and Jurkats. Our immunofluorescence results also show that the purification protocol yields purified nuclei with intact nuclear envelope as shown with Sun2 staining (Figure 3B). Nuclei also retain dynein on the NE as shown with p150Glued staining (Figure 3E). We also showed that isolated nuclei can establish stronger interaction with MTs when competed with kinesin-1 coating (Figure 5A). To show the reproducibility of the reconstitution assay, we also recapitulated MT-nucleus interaction in different adherent cell nuclei purified with different protocol (Figure 4). Overall, we were able to reconstitute MT-nucleus interaction in various non-adherent cell types and create a biochemical balance where nucleus and MTs were able to survive and interact.

It has been shown that nuclear-bound dynein transfers MT forces on the nucleus (Levy and Holzbaur, 2008; Zhou et al., 2009; Fridolfsson et al., 2010). As dynein was present on purified HSC and Jurkat NE (Figure 3E), we hypothesized that reconstitution of MT-nucleus interaction could lead to nucleus deformation upon MT-strangling. Indeed, nuclear-bound dynein has been shown to transfer MT forces on and deform the nucleus (Biedzinski et al, 2020). However, during live-imaging, we did not observe any nuclear deformations despite the presence of dynein and MTs. This result might imply that dynein motors are not functional despite their presence. Further work should be considered to better preserve the motor activity. The reconstitution buffer couldn't have been the limitation on dynein activity, because the biochemical conditions were compatible for kinesin-1 functioning as confirmed with MT gliding (Figure XX). Therefore the damage on dynein functionality likely happened in an earlier step during mechanical shearing (Figure XX). This is also the step where centrosome-bearing nuclei number sharply decreased by 85% (Figure XX). With further optimization, this assay would allow to reproduce nucleus deformation and study how it impacts lamin localization, chromatin remodeling, modulation of transcription, nuclear pore complex (NPC) positioning on NE, DSB repair, or any other specific process that could be downstream of MT-nucleus interactions.

REFERENCES (are not listed by numbers in the text yet, i will let manuel see it with the initial version first)

4. Almonacid M, Al Jord A, El-Hayek S, Othmani A, Coulpier F, Lemoine S, Miyamoto K, Grosse R, Klein C, Piolot T et al (2019) Active fluctuations of the nuclear envelope shape the transcriptional dynamics in oocytes. Dev Cell 51: 145 – 157.e10
5. Beaudouin J, Gerlich D, Daigle N, Eils R, Ellenberg J (2002) Nuclear envelope breakdown proceeds by microtubule-induced tearing of the lamina. Cell 108: 83 – 96
6. Biedzinski et al. 2020 EMBO J
7. Cadot B, Gache V, Vasyutina E, Falcone S, Birchmeier C, Gomes ER (2012) Nuclear movement during myotube formation is microtubule and dynein dependent and is regulated by Cdc42, Par6 and Par3. EMBO Rep 13:741 – 749
8. Cavazza et al, 2020 BioRxiv
9. Chakraborty et al 2018 Meth in Cell Bio
10. Davidson & Cadot 2020 Trends in Cell Bio
11. Fridolfsson HN, Ly N, Meyerzon M, Starr DA. 2010. UNC-83 coordinates kinesin-1 and dynein activities at the nuclear envelope during nuclear migration. Dev Biol 338:237–250.
12. Gache et al, 2017 MBoC
13. Guilluy et al. 2014 NCB
14. Gupta S, Marcel N, Sarin A, Shivashankar GV (2012) Role of actin dependent nuclear deformation in regulating early gene expression. PLoS ONE 7: e53031
15. Inoue et al. 2019 EMBO J
16. Levy JR, Holzbaur EL. 2008. Dynein drives nuclear rotation during forward progression of motile fibroblasts. J Cell Sci 121:3187–3195.
17. Lottersberger et al. 2015 Cell
18. Majumder et al. 2019 JCS

19. Metzger T, Gache V, Xu M, Cadot B, Folker ES, Richardson BE, Gomes ER, Baylies MK (2012). MAP and kinesin-dependent nuclear positioning is required for skeletal muscle function. Nature 484, 120–124.
20. Nastaly et al 2020 Nat Comm
21. Olins & Olins 2004 BMC Cell Biology
22. Pierce, D. W. & Vale, R. D. Assaying processive movement of kinesin by fluorescence microscopy. Methods Enzymol. 298, 154–171 (1998).
23. Procter et al. 2020 Nature
24. Prosser & Pelletier 2017 Nat Rev MCB 2017
25. Reinsch S, Gönczy P (1998) Mechanisms of nuclear positioning. J Cell Sci 111: 2283–2295
26. Renkawitz, J., Kopf, A., Stopp, J. *et al.* Nuclear positioning facilitates amoeboid migration along the path of least resistance. *Nature* **568,** 546–550 (2019).
27. Schaedel et al. 2019 Nat Physics
28. Starr DA, Fridolfsson HN (2010) Interactions between nuclei and the cytoskeleton are mediated by SUN-KASH nuclear-envelope bridges. Annu Rev Cell Dev Biol 26: 421–444
29. Tassin AM & Maro B, Bornens M (1985) Fate of microtubule-organizing centers during myogenesis in vitro. J Cell Biol 100: 35–46
30. Triclin et al. 2021
31. Yajima et al 2012 JCB
32. Zhou K, Rolls MM, Hall DH, Malone CJ, Hanna-RoseW. 2009. A ZYG-12-dynein interaction at the nuclear envelope defines cytoskeletal architecture in the C. elegans gonad. J Cell Biol 186:229–241.
33. references number 40, 41, 42 from Laura's paper for tubulin purification and labeling.

modified biblio (numbers are not matching for now):

Brinkmann V, Reichard U, Goosmann C, Fauler B, Uhlemann Y, Weiss DS, et al. Neutrophil extracellular traps kill bacteria. *Science* (2004) 303:1532–5.

S. Barzilai, S.K. Yadav, S. Morrell, F. Roncato, E. Klein, L. Stoler-Barak, O. Golani, S.W. Feigelson, A. Zemel, S. Nourshargh, *et al.*Leukocytes breach endothelial barriers by insertion of nuclear lobes and disassembly of endothelial actin filaments Cell Rep., 18 (2017), pp. 685-699.

PajerowskiJD, DahlKN, ZhongFL, SammakPJ, DischerDE, 2007. Physical plasticity of the nucleus in stem cell differentiation. *PNAS* 104:15619–24.

Stephens et al. 2017 MBOC Chromatin histone modifications and rigidity affect nuclear morphology independence of lamins.

Zink D, Fischer AH, Nickerson JA (2004) Nuclear structure in cancer cells. Nat Rev Cancer 4(9):677–687.

Thiam, H. R. et al. Perinuclear Arp2/3-driven actin polymerization enables nuclear deformation to facilitate cell migration through complex environments. Nat. Commun. 7, 10997 (2016).

Teresa Sullivan, Diana Escalante-Alcalde, Harshida Bhatt, Miriam Anver, Narayan Bhat, Kunio Nagashima, Colin L. Stewart, Brian Burke; Loss of a-Type Lamin Expression Compromises

Nuclear Envelope Integrity Leading to Muscular Dystrophy. *J Cell Biol* 29 November 1999; 147 (5): 913–920.

Scaffidi and Misteli, 2006

Hoffmann et al, 2002

Maro & Bornens, 1980

(CADOT REFERENCE Dean & Kasamatsu, 1994 JBC)

Author Contributions

GA: designed most and performed all experiments. wrote the manuscript with inputs from all authors.

BC: performed myotube and myoblast experiments with GA.

JG: performed the tubulin purifications, fluorescent labeling and buffer characterization.

LB: designed and conducted the study.

EF: designed and conducted the study.

MT: designed and conducted the study.